

# ENGINEERING SURFACE ROUGHNESS TO MANIPULATE DROPLETS IN MICROFLUIDIC SYSTEMS

Ashutosh Shastry, Marianne J. Case and Karl F. Böhringer

Department of Electrical Engineering, University of Washington, Seattle, USA

## ABSTRACT

Systematic variation of surface roughness has been employed to create microstructured guide rails for droplets propelled by vibration. The wetting mechanism of rough hydrophobic surfaces has been utilized to design surface energy gradients that form the guide-rails. Microfabricated pillars in silicon have been employed to control the roughness which determines the contact angle and thus the surface energy. Droplets were moved down the surface energy gradient overcoming hysteresis by supplying energy through mechanical vibration. This work introduces roughness as a new control variable in any scheme of manipulating droplets, and presents fabricated structures and experimental results that validate the approach.

## 1. INTRODUCTION

Microscale bioanalysis is pregnant with assay possibilities both for diagnostic applications and also for understanding new biology. Continuous flow systems have been the default approach towards such lab-on-chip bioassay systems. However, droplet based lab-on-chip applications have become increasingly popular because of their ability to enable spatially and temporally resolved chemistries [1]. Employing surface energy gradients to cause movement of droplets has been a common theme of several apparently disparate actuation approaches. Actuations using Maragoni effects [2], electrowetting effects [3] and those due to a contact angle gradient created by varying chemical composition [4, 5] have been reported in the past. These different surface forces scale favorably in the micro-domain and present an attractive proposition for manipulating droplets in the microfluidic environment.

In the last few years, there have been remarkable advances in the understanding of wetting of rough surfaces [6]. This understanding opens up the possibilities of employing roughness as a new candidate control variable that can be engineered to participate in the manipulation of droplets.

## 2. THEORY AND DESIGN

We begin by reviewing the theory of wetting of rough surfaces. Based on this theory, we then detail our approach for designing surface energy gradients.

## Wetting of Rough Surfaces

Let us imagine a structured rough surface formed by constructing pillars of controlled geometry on a smooth surface. The basic effect of surface roughness can be easily understood by the Wenzel equation [7], which relates the apparent contact angle  $\theta_w$  of a drop on a rough surface with roughness  $r > 1$ . Here,  $r$  is the ratio of rough to planar surface areas, as explained in Fig. 1, and can be related to Young's intrinsic contact angle  $\theta_i$  by the following equation:

$$\cos \theta_w = r \cos \theta_i$$

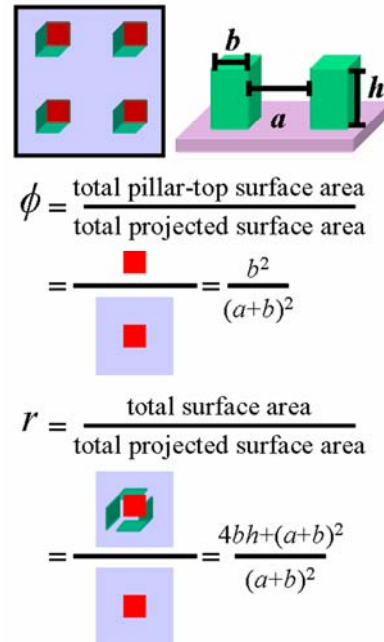


Figure 1. Surface texture parameters to quantify roughness of a surface.

The apparent contact angle of a sessile droplet varies not only with physical texture or the roughness but also with the chemical texture determined by the composition of the solid surface. Consider a chemically heterogeneous surface [7] made up of two different chemical species characterized by their intrinsic contact angles  $\theta_{i,1}$  and  $\theta_{i,2}$ , respectively. The individual areas are assumed to be much smaller than the drop size and let  $\phi_1$  and  $\phi_2$  be the area fraction of each of the species ( $\phi_1 + \phi_2 = 1$ ). The apparent contact angle in this case is named after Cassie-Baxter and is given by the equation as follows:

$$\cos \theta_{cb} = \phi_1 \cos \theta_{i,1} + \phi_2 \cos \theta_{i,2}$$

A droplet can sit on a solid surface in two distinct configurations or states (Fig. 2). It is said to be in Wenzel state when it is conformal with the topography. Wenzel's equation explained earlier is used to compute the apparent contact angle. The other state in which a droplet can rest on the surface is called the Fakir state, where it is not conformal with the topography and only touches the tops of the protrusions on the surface.

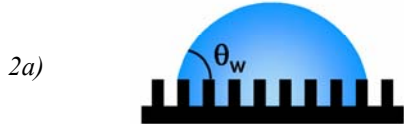


Figure 2(a): Schematic drawing to show the cross-section of a drop making Wenzel contact with a rough surface [9].

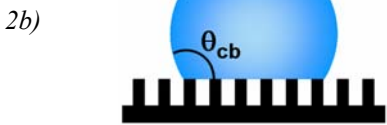


Figure 2(b): Schematic drawing to show the cross-section of a drop making Fakir contact with a rough surface [9].

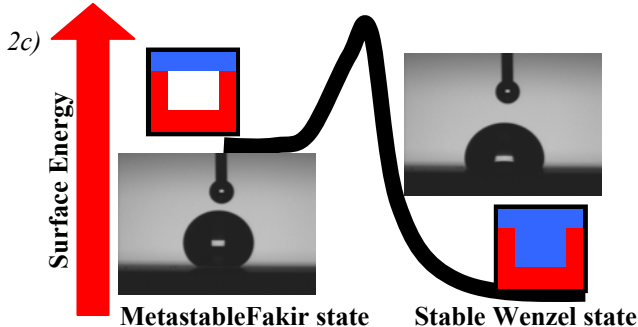


Figure 2(c): Schematic drawing to show the energy barrier that stabilizes the metastable Fakir state.

This leads to the formation of a composite surface with trapped air pockets. The Cassie-Baxter relationship from the previous equation is therefore employed to determine the apparent contact angle in the Fakir state. The solid surface has an area fraction of  $\phi$  and an intrinsic contact angle of  $\theta_i$ ; the freely suspended fraction contacting air has an area fraction of  $(1-\phi)$  and a contact angle of  $180^\circ$ . Substituting the values, the apparent contact angle in the Fakir state is readily computed as [6]:

$$\cos \theta_{cb} = \phi(\cos \theta_i + 1) - 1$$

The Fakir or the air-pocket state is stable if the following inequality holds true:

$$\cos \theta_i < \frac{\phi - 1}{r - \phi}$$

For a given material, thus having fixed  $\theta_i$ , this state could be stable or "metastable" depending on the choice of the parameters  $r$  and  $\phi$ . Here, metastable and stable are

analogous to local and global energy minima; but clearly very distinct from them. While a local and a global minimum, if they are distinct, have different locations in space, a stable and a metastable state correspond to two different energy levels at the same location; metastable corresponding to the higher energy level. So when a droplet is in Fakir state and the Wenzel state at that location in space has a lower energy, then the Fakir state is the metastable state while Wenzel is the stable state. The reason why a droplet does not spontaneously transit to the lower energy Wenzel state is because of the presence of an energy barrier; analogous to the activation energy of a reaction that prevents spontaneous conversion to products (Fig. 2(c)). The energy barrier thus accounts for the meta-stability and is easily estimated [8]. It gives a useful bound on the energy that needs to be coupled to the droplet before one risks its transition to the stable Wenzel state.

### Surface Design

We have developed chemically homogeneous but textured surfaces. A regular two-dimensional array of square pillars created a rough surface with controlled roughness parameters  $\phi$  and  $r$ . Pillar width  $b$ , height  $h$  and spacing  $a$  defined  $\phi$  and  $r$ , explained in Fig. 1. A set of  $a$ ,  $b$  and  $h$  defined a roughness and a corresponding apparent contact angle as given by the Cassie-Baxter equation for the Fakir state described earlier.

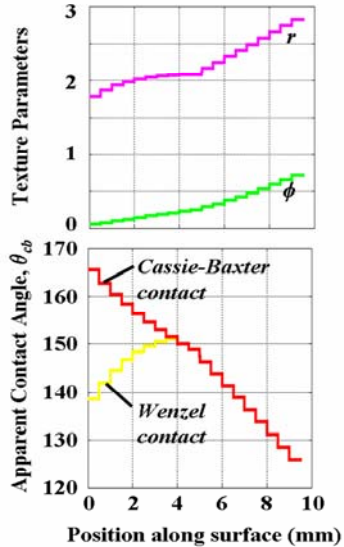


Figure 3. Designed  $\phi$ ,  $r$  and apparent contact angle  $\theta_{cb}$  profiles along the die used in our experiments.

A gradient track that guides the droplet is essentially a series of contiguous strips of different roughness values. Each step seen in Fig. 3 corresponds to one such roughness value and the pillar parameters  $a$ ,  $b$  and  $h$  are kept constant over a strip. The strip width is constrained by two competing requirements. It needs to be wide enough with sufficient rows of pillars to justify the use of an average  $\phi$  and  $r$  for the strip. For the droplet to experience the surface energy gradient, the roughness

strips need to be narrow enough so that a droplet contacts at least two strips at all times. By corollary, for this approach to be employed for very small droplets, the requirement that the pillar dimensions need to be roughly one order of magnitude smaller than the droplet size could determine the limit of scalability.

For one of the dies,  $\phi$  increased every 500 microns along the surface, creating an apparent contact angle gradient shown in Fig. 3. As seen in this plot, there exists a bifurcation at approximately position 4mm that divides the die into two distinct regions. The high contact angle region to the left has two possible states of the droplet at each x-coordinate while the region to the right has only one possible state for each location. In the left region, the Fakir state is only metastable and given sufficient energy, the droplet can transit to the lower energy Wenzel state. In the region to the right, the Fakir is the most stable state and there is no risk of the droplet transiting to the higher energy Wenzel state. Ideal choice of parameters would be such that the right region spanned the entire length of the die and there were no risk of the droplet transiting to the Wenzel state. However, this security would limit the choice of pillar dimensions and would be at the cost of steepness of the gradient. A stipulated gradient can be achieved in multiple ways. Several gradients were designed and different combinations were tried to realize a particular gradient. The plot shown is representative of a healthy compromise between the steepness, span and fabrication constraints. Our current DRIE process allowed a maximum aspect ratio of 1:5. It meant a minimum dimension of 16 micron  $\times$  16 micron for a height of 88 microns. As the pillar dimensions get smaller, the allowed pillar height also gets smaller and so does the energy barrier for transition. A low  $\phi$  is expected to reduce the hysteresis and thereby lower the energy required for actuation. The lowered energy barrier could therefore still suffice. A thorough exploration of this design space is under way.

### 3. FABRICATION

Masks were made in L-Edit with the pillar dimensions  $b$  and  $a$  varying at regular intervals to translate the designed gradients into pillar arrays. A typical mask of a gradient surface is shown in Fig. 4(a). Standard photolithography with AZ4620 resist was followed by a DRIE Bosch® process to etch pillars in an n-type <100> silicon substrate. The height of the pillars  $h$  specified the etch depth. Following photolithography, the resist was stripped and the wafers were cleaned and diced. Fig. 4(c) shows the die at this stage. Each die was individually spin-coated with silane, an adhesion promoter for Teflon AF, and cured.

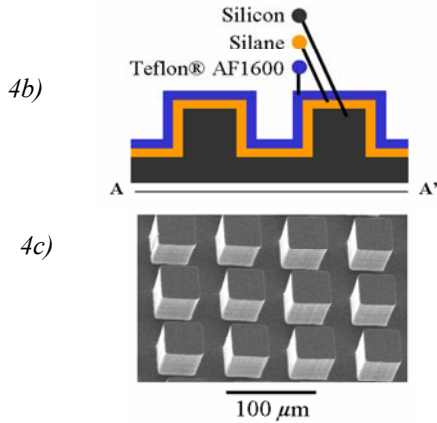
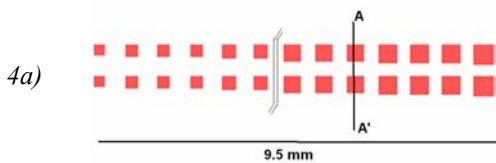


Figure 4. Microfabricated surface texture gradient.  
a) Top view.  
b) Sectional side view.  
c) SEM micrograph of the die.

Finally the dies were spin coated with Teflon® AF1600, dried and cured. Fig. 4(b) shows the schematic cross-section of a test die. At this stage, the die is ready to be mounted on the test platform for the experiments.

### 4. EXPERIMENTAL RESULTS

The test die was mounted on a glass slide with double-sided tape and placed in the observation setup detailed in Fig. 5. The slide was glued onto a stage attached to a speaker diaphragm. The assembly was kept under a microscope fitted with a CCD camera. Care was taken to ensure that the die was perfectly horizontal to minimize biasing due to gravity. The droplet was dispensed near the left edge of the test die where the apparent contact angle was high and set in motion by vibrating the speaker. A square wave of 60 Hz and varying amplitudes was used. Fig. 6(a) shows the droplet movement.

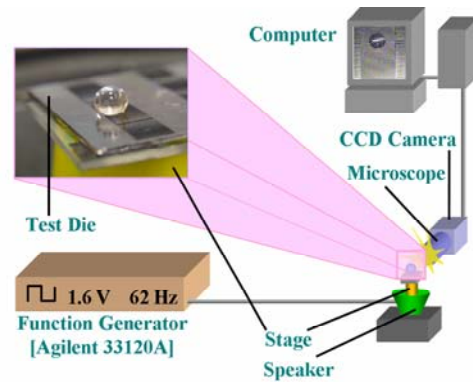
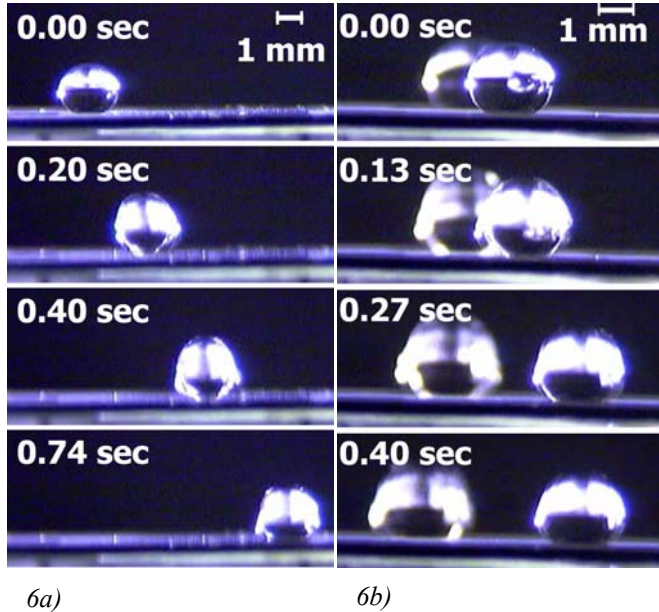


Fig. 5. Actuation and observation setup.

Any impending motion of the droplet is opposed by contact angle hysteresis. Hysteresis results from the pinning of the three-phase contact line to the solid surface, which is attributed to physical and chemical inhomogeneities [7]. Vibration supplies kinetic energy to

the droplet to mitigate this hysteresis and to allow movement while retaining the Fakir state.



*Fig. 6a) Vibration causes the droplet to travel down a gradient.*

*b) Die with identical gradients in opposite directions was vibrated. Each gradient served as control for the other. This proved that the droplet was guided by the gradients and not by bias in vibration or gravity.*

Control experiments were done with gradients oriented in opposite directions on a die and it was conclusively established that the drop moved down the surface energy gradient. A sample control experiment is shown in Fig. 6(b).

### Droplet Velocity vs. Position

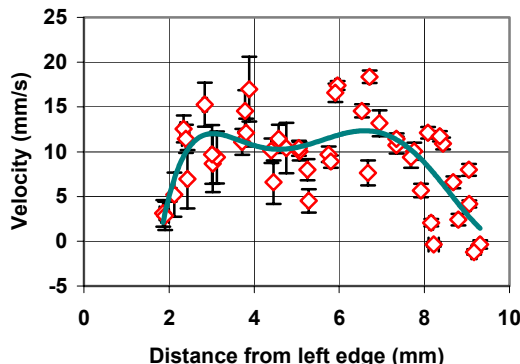


*Fig. 7. The scatter plot sums up four runs with a square wave of 1V pk-pk at 54 Hz. The dip in velocity in the middle correlates to a decrease in the gradient at that point as seen in the design plot of Fig. 3.*

The gradient thus provides a ratcheting effect and rectifies the motion caused by vibration. A frame-by-frame analysis of the droplet position from the video-recorded

images yields the velocity of droplet migration shown in Fig. 7.

The higher hysteresis in the Wenzel state is readily explained by a much higher solid liquid contact area than in the Fakir state, offering proportionally higher surface inhomogeneities to cause pinning. Extending the same argument, even within Fakir state, the hysteresis is expected to increase as the solid-liquid contact area fraction  $\phi$  increases. This expectation was confirmed by two experimental observations: (1) The droplet traversed progressively smaller distances as the actuation voltage was reduced. (2) For a given frequency and amplitude, the velocity decreased towards the right end of the die (Fig. 7).

### 5. CONCLUSIONS

This work provides design rules for exploiting physical texture to create surface energy gradients that guide droplets along desired trajectories. Based on this static analysis, further experimental investigation is required to understand better the hysteresis and dynamics of moving droplets in microfluidic systems.

### ACKNOWLEDGEMENTS

This work is funded by NIH Center of Excellence in Genomic Science and Technology grant 1-P50-HG002360-01.

### REFERENCES

- [1] H. A. Stone, A. D. Stroock, and A. Ajdari, "Engineering Flows in Small Devices: Microfluidics Toward a Lab-on-a-Chip", *Ann. Rev. Fluid Mech.*, vol. 36, pp. 381–411, 2004.
- [2] A. A. Darhuber, J. P. Valentino, J. M. Davis, S. M. Troian and S. Wagner, "Microfluidic actuation by modulation of surface stresses", *App. Phys. Lett.*, vol. 82, no. 4, pp. 657-659, 2003.
- [3] M. Pollack, R. Fair, and A. Shenderov, "Electrowetting-based actuation of droplets for integrated microfluidics", *Lab on a Chip*, vol. 2, pp. 96–101, 2002.
- [4] M. K. Chaudhury and G. M. Whitesides, "How to make water run uphill?", *Science*, vol. 256, no. 5063, pp. 1539-1541, 1992.
- [5] S. Daniel, S. Sircar, J. Gliem, and M. K. Chaudhury, "Ratcheting Motion of Liquid Drops on Gradient Surfaces", *Langmuir*, vol. 20, pp. 4085-4092, 2004.
- [6] J. Bico, U. Thiele, and D. Quéré, "Wetting of textured surfaces", *Colloids and Surfaces A: Physicochemical and Engineering Aspects*, vol. 206, pp. 41–46, 2002.
- [7] P. G. de Gennes, F. Brochard-Wyart, and D. Quéré, *Capillarity and Wetting Phenomena: Drops, Bubbles, Pearls, Waves*, Springer, 2004.
- [8] N.A. Patankar, "Transition between Superhydrophobic States on Rough Surfaces", *Langmuir*, vol. 20, pp. 7097-7102, 2004.
- [9] J. Bico, C. Tordeux, and D. Quéré, "Rough Wetting," *Europhysics Letters*, vol. 55, no. 2, pp. 214–220, 2003.